Network inference using asynchronously updated kinetic Ising model

Hong-Li Zeng,[1,*] Erik Aurell,[2,3] Mikko Alava,[1] and Hamed Mahmoudi[3]

[1]*Department of Applied Physics, Aalto University, FIN-00076 Aalto, Finland*
[2]*Linnaeus Centre, KTH-Royal Institute of Technology, S-100 44 Stockholm, Sweden*
[3]*Department of Information and Computer Science, Aalto University, FIN-00076 Aalto, Finland*

Network structures are reconstructed from dynamical data by respectively naive mean field (nMF) and Thouless-Anderson-Palmer (TAP) approximations. TAP approximation adds simple corrections to the nMF approximation, taking into account the effect of the focused spin on itself via its influence on other neighboring spins. For TAP approximation, we use two methods to reconstruct the network: (a) iterative method; (b) casting the inference formula to a set of cubic equations and solving it directly. We investigate inference of the asymmetric Sherrington-Kirkpatrick (aS-K) model using asynchronous update. The solutions of the set of cubic equations depend on temperature T in the aS-K model, and a critical temperature $T_c \approx 2.1$ is found. The two methods for TAP approximation produce the same results when the iterative method is convergent. Compared to nMF, TAP is somewhat better at low temperatures, but approaches the same performance as temperature increases. Both nMF and TAP approximation reconstruct better for longer data length L, but for the degree of improvement, TAP performs better than nMF.

PACS number(s): 02.50.Tt, 02.30.Mv, 89.75.Fb, 87.10.Mn

I. INTRODUCTION

A present challenge in biological research is how to deal with the data originating from the high-throughput technologies. However, network theory provides a path to structure the information. Vertices on a network are entities and the links with numbers or other descriptions attached to them are the interactions between the elements, for example, in the biological system [1–5]. On different levels of abstraction, information about the interactions between element pairs is hence useful to understand the biological system. As in [6], with distinct types of data, the challenge is to discover gene modules and interactions between the modules computationally. Finding interactions between entities from observable data is an inverse problem called "network reconstruction." Many approaches have been developed to unveil the underlying network topology, like iterative reverse engineering method [7,8] and correlation-based method [9–12].

In this work, we use an idealized system to generate "empirical" data with a computer and then try to reconstruct the network structure of the system using these test data. With a precisely known network, the assessments and comparisons of inference algorithms, as in [13,14], are feasible. The system is the kinetic Ising model, intended as a proxy for simultaneous recordings from many neurons. The model is called "kinetic" because, except for the fully symmetric case, it does not correspond to an equilibrium statistical mechanics system. In this setting, symmetric couplings between the entities are not appropriate, as two neurons typically do not act on each other in a symmetric way [15]. The properties of asymmetric neural networks have been studied previously [16–18], but not much work has been done in the context of network reconstruction.

Here we extend a presently reported approach using dynamic mean field theory [19,20] from synchronously updated models to asynchronously updated models. The analysis closely parallels that of [20], with the difference that data are continuous in time. There are several reasons to consider the asynchronous case instead of the synchronous case. First, asynchronous updates converge to a stationary state which for symmetric models is the Boltzmann-Gibbs equilibrium measure, while this is not necessarily true for a synchronous case. A second reason is that most plausible applications are naturally asynchronous. For instance, the expression of gene is not a synchronous process; the transcription of DNA and the transport of enzymes may take from milliseconds up to a few seconds. The refractory period for neuron is that in which the neuron cannot respond to an input signal because it is still processing or recovering from the previous input signal [21]. It generally lasts for 1 ms in a neuron. Besides, studies in [22,23] expect that the biological networks do not have a completely synchronous update. Thus, we focus on the asynchronous update Glauber dynamics.

Multineuron firing patterns can be observed with present technologies up to thousands of neurons (recordings on retina systems). Schneidman *et al.* [24] showed that the interactions between neuron pairs could be reconstructed using only the observed firing rates and the pairwise correlations. Recently, questions have arisen whether the methods used in [24] generalize to other data sets and if the approximations involved can be improved [9–12]. There has also been significant development on the more theoretical side [9,25–27].

A theoretical model, which can be used to generate the frequencies of all possible spiking configurations, is the well-known Ising model [9]. For a system of N neurons, it is characterized by up to N^2 parameters: N external fields, θ_i, on each individual neuron, and $N(N-1)$ "links," J_{ij}, between each pair of neurons. In an asymmetric Sherrington-Kirkpatrick (aS-K) model, J_{ij} is not equal to J_{ji}.

With the observed average firing rates and all pairwise equal-time correlations in an empirical data set, maximum entropy models can find a probability distribution which maximizes the entropy of the data domain. This condition

_____
*hongli.zeng@tkk.fi

implies that the samples are drawn independently from the same distribution. The state given maximum entropy is an equilibrium state which has a probability distribution of Ising form [28]. The quantities J_{ij} and h_i are then Lagrange multipliers to satisfy the constraints that the ensemble expectation values agree with sample averages in the data set. However, if the data is generated by a dynamics, then samplings drawn close in time are typically dependent. This is the extra information which will be used here through the kinetic inverse Ising reconstruction scheme. For the equilibrium version of the inverse Ising problem, Roudi and collaborators review and investigate several approximation methods [10,11,27] with the maximum entropy method, arriving at the general conclusion that all of them are unreliable in a dynamic setting, if the systems are sufficiently large, and in most ranges of parameters. Better inference methods on dynamic data are called for.

A standard approach to sample the equilibrium Ising model is Glauber dynamics [29,30], which we describe below. It is, however, not restricted to symmetric Ising model, but also well-defined for models with asymmetric couplings. It is plausible that such a more general framework can describe the underlying system not close to equilibrium and, with asymmetric couplings, describe it better. Here we are therefore interested in using a kinetic Ising model, typically with asymmetric couplings, to reconstruct a neural network dynamically.

The paper is organized as follows: We describe the aS-K model and Glauber dynamics in Sec. II; the inference formula with naive mean field (nMF) and Thouless-Anderson-Palmer (TAP) approximation for the asynchronous case is derived in Sec. III; the performances of the inference formula are given in Sec. IV. Finally, we summarize the work in Sec. V.

II. ASYMMETRIC S-K MODEL AND GLAUBER DYNAMICS

The aS-K model is a system of N spins, which models N neurons with binary states ($s_i = 1$ for firing state; otherwise $s_i = -1$). It is a fully connected model; that is, all neurons in the system have interactions with each other. The interactions J_{ij} between each pair of neurons have the following form:

$$J_{ij} = J_{ij}^s + k J_{ij}^{\text{as}}, \quad k \geqslant 0, \tag{1}$$

where k measures the asymmetric degree of these interactions, J_{ij}^s and J_{ij}^{as} are symmetric $J_{ij}^s = J_{ji}^s$ and asymmetric $J_{ij}^{\text{as}} = -J_{ji}^{\text{as}}$ matrices, respectively. They both consist of identically and independently Gaussian distributed random variables with means 0 and variances:

$$\langle J_{ij}^{s\,2} \rangle = \langle J_{ij}^{\text{as}\,2} \rangle = \frac{J^2}{N} \frac{1}{1 + k^2}. \tag{2}$$

The self-connections are avoided; that is, the on-diagonal elements of J_{ij}^s and J_{ij}^{as} equal 0.

We now define the kinetic Ising model with asynchronous updates. Let the joint probability distribution of spin states in

system at time t be $p(s_1,...,s_N;t)$, and let the master equation of our model be written as

$$\frac{d}{dt} p(s_1,...,s_N;t) = \sum_i \omega_i(-s_i) p(s_1,..., -s_i,...,s_N;t)$$
$$- \sum_i \omega_i(s_i) p(\mathbf{s};t), \tag{3}$$

where $\omega_i(s_i)$ is the flipping rate; that is, the probability for the state of ith neuron changes from s_i to $-s_i$ per unit time. The flipping rates are given by Glauber dynamics as follows:

$$\omega_i(s_i) = \frac{1}{1 + \exp\left[2\beta s_i\left(\theta_i + \sum_j J_{ij} s_j\right)\right]}, \tag{4}$$

where, β is the inverse of temperature T. For convenience, define $H_i = \sum_j J_{ij} s_j + \theta_i$ as the effective field on neuron i, where θ_i is the external field of spin i. If the couplings are symmetric (i.e., $J_{ij}^{\text{as}} = 0$), then the steady state of the dynamics given by Eqs. (3) and (4) is $p(s_1,...,s_N) \propto \exp(\beta \sum_i s_i \theta_i + \sum_{ij} s_i s_j J_{ij})$. If the couplings are not symmetric, then Eqs. (3) and (4) still have a steady state (under general condition), but this state does not have a simple description.

With state for each neuron s_i, we can naturally define the time-dependent means and correlations as follows:

$$m_i = \langle s_i(t) \rangle;$$
$$C_{ij}(t - t_0) = \langle s_i(t) s_j(t_0) \rangle - m_i m_j. \tag{5}$$

From Eqs. (3) and (4), we get the equations of motion for means and correlations as

$$\frac{dm_i}{dt} = -m_i + \langle \tanh[\beta s_i H_i(t)] \rangle.$$
$$\tag{6}$$
$$\frac{d}{dt} \langle s_i(t) s_j(t_0) \rangle = -\langle s_i(t) s_j(t_0) \rangle + \langle \tanh[\beta H_i(t) s_j(t_0)] \rangle.$$

For the second equation of Eq. (6), the term on the left-hand side and the first term on the right-hand side can be solved based on the empirical data produced by the Glauber dynamics. However, the calculation of the average value for $\tanh[\beta H_i(t) s_j(t_0)]$ involves all kinds of higher-order correlations and is therefore not easily expressed only in terms of means and pairwise correlations. In order to solve the second equation in (6), perturbative approximations for the second term of the right-hand side are obviously needed. Here we use the nMF and TAP approximations, respectively, to deal with this tanh function.

III. NMF APPROXIMATION AND TAP APPROXIMATION

The simplest method to find out the parameters of the Ising model from empirical data is the mean-field theory:

$$m_i = \tanh \beta \left(\theta_i + \sum_j J_{ij} m_j \right). \tag{7}$$

Following recent practice, and to distinguish this first level of approximation from others, we refer to it as naive mean field (nMF). Let $b_i = \theta_i + \sum_j J_{ij} m_j$ and rewrite H_i as

$$H_i = b_i + \sum_j J_{ij}(s_j - m_j) \equiv \sum_j J_{ij} \delta s_j + b_i. \tag{8}$$

Expanding the tanh function with respect to βb_i in Eq. (6),

$$\frac{d}{dt}\langle s_i(t)s_j(t_0)\rangle + \langle s_i(t)s_j(t_0)\rangle = m_i m_j + \beta\left(1 - m_i^2\right)$$
$$\times \left(\sum_k J_{ik}\langle \delta s_k(t)\delta s_j(t_0)\rangle\right),$$
(9)

and denoting the time difference $t - t_0$ as τ, we have

$$\frac{d}{d\tau}C_{ij}(\tau) + C_{ij}(\tau) = \beta\left(1 - m_i^2\right)\sum_k J_{ik}C_{kj}(\tau). \quad (10)$$

In the limit $\tau \to 0$, we obtain the equation which we need to infer the network couplings:

$$J = TA^{-1}DC^{-1}, \quad (11)$$

where $D = \dot{C} + C$ and $A_{ij} = \delta_{ij}(1 - m_i^2)$.

Equation (11) is a linear matrix equation with respect to J_{ij}. We can solve it directly.

Next, we turn to derive the inference formula with TAP [31] approximation. If the Onsager term, that is, the effect of the mean value of neuron i on itself via its influence on another neuron j, is taken into account, then the TAP equation can be obtained as [32,33]

$$m_i = \tanh\left(\beta b_i - m_i\beta^2\sum_{k\neq i}J_{ik}^2\left(1 - m_k^2\right)\right). \quad (12)$$

With

$$T_i = b_i \pm m_i\beta^2\sum_{k\neq i}J_{ik}^2\left(1 - m_k^2\right) + \sum_j J_{ik}\delta s_k. \quad (13)$$

and Eq. (12), we expand the tanh function in Eq. (6) with respect to

$$\beta b_i - m_i\beta^2\sum_{k\neq i}J_{ik}^2\left(1 - m_k^2\right)$$

to the third order and keep the terms only up to the third order of **J**. Then the corresponding TAP inference formula for J_{ij} is obtained, which is formally the same as in the nMF approximation:

$$J = TA^{-1}DC^{-1}. \quad (14)$$

However, matrix **A** in a TAP formula is different:

$$A_{ij} = \delta_{ij}\left(1 - m_i^2\right)\left[1 - \beta^2\left(1 - m_i^2\right)\sum_j J_{ij}^2\left(1 - m_j^2\right)\right]. \quad (15)$$

Equation (14) is a function of the couplings **J**, and therefore it is a nonlinear equation for matrix **J**.

We try to solve Eq. (14) for **J** though two approaches. One way is to solve it iteratively. We start from reasonable initial values J_{ij}^0 and insert them in the right-hand side of the formula. The resulting J_{ij}^1 is the solution after one iteration. This can be again replaced in the right-hand side to get the second iteration results, etc.,

$$J^{t+1} = TA^{-1}(J^t)DC^{-1}. \quad (16)$$

An alternative way is to solve it directly, as done for the synchronous update model in [20], casting the inference formula to a set of cubic equations. For Eq. (15), we denote

$$F_i = \beta^2\left(1 - m_i^2\right)\sum_j J_{ij}^2\left(1 - m_j^2\right) \quad (17)$$

and plug it into Eq. (14), and then obtain the following equation for J_{ij}:

$$J_{ij}^{\text{TAP}} = \frac{T * V_{ij}}{(1 - m_i^2)(1 - F_i)}, \quad (18)$$

where $V_{ij} = [DC^{-1}]_{ij}$. Inserting Eq. (18) into Eq. (17), we obtain the cubic equation for F_i as

$$F_i(1 - F_i)^2 - \frac{\sum_j V_{ij}^2\left(1 - m_j^2\right)}{1 - m_i^2} = 0. \quad (19)$$

With the obtained physical solution for F_i, we get the reconstructed couplings J^{TAP} as

$$J_{ij}^{\text{TAP}} = \frac{J_{ij}^{\text{nMF}}}{1 - F_i}. \quad (20)$$

It is worth mentioning that for the cubic equation (18), we have three solutions with possible imaginary parts. Here we study the real roots of the cubic equation and ignore those solutions with imaginary parts. When three solutions are all real ones, we take the smallest one.

We introduce Δ to measure the difference between the reconstructed network structure and the original true ones; that is, Δ is the reconstruction error

$$\Delta = \sqrt{\frac{\sum_{i\neq j}\left(J_{ij}^{\text{re}} - J_{ij}^{\text{true}}\right)^2}{\sum(J_{ij}^{\text{true}})^2}},$$

where J_{ij}^{true} represents the true network couplings and J_{ij}^{re} for the reconstructed ones.

IV. THE PERFORMANCES OF NMF AND TAP APPROXIMATION

As the starting point, we take a look at the number of solutions given by nMF and TAP approximation. The nMF gives a unique solution while the iteration method of TAP starting from nMF provides 0 solution when the iteration is divergent and 1 solution for convergence. However, the cubic-equation method of TAP approximation always contains at least one solution. We denote the constant term of Eq. (19) as x,

$$x = -\frac{\sum_j V_{ij}^2\left(1 - m_j^2\right)}{\left(1 - m_i^2\right)}. \quad (21)$$

x is temperature dependent and negative as $0 < m_i^2 < 1$. The cubic equation (19) has three real roots when $-\frac{4}{27} < x < 0$. We only consider the smallest one and indeed it provides the most accurate J_{ij}'s (data are not shown). With $x < -\frac{4}{27}$, Eq. (19) has only one real root and other two complex solutions with imaginary part which are discarded as they have no physical meaning. In Fig. 1, we give the fraction of cubic-equation set (19) (as $i = 1,2,...,N$, where N is the
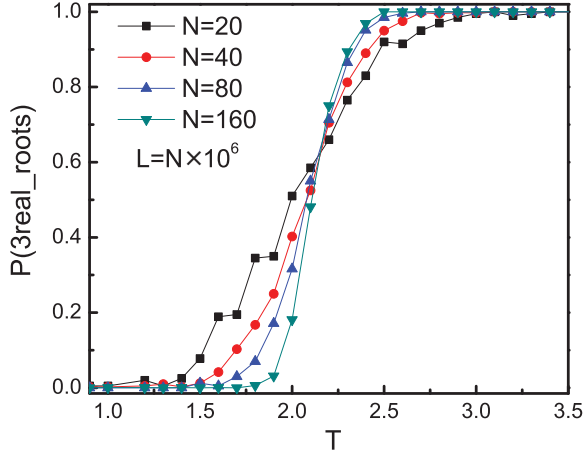
FIG. 1. (Color online) The fraction of three real roots for the cubic equation set Eq. (19). A transition seems to occur around $T_c = 2.1$. Here we find larger N, the transition curve sharper. The parameter values: $\theta = 0.5$, $k = 1$, $L = 20 \times 10^6$.

system size), which contains three real solutions. When the cubic-equation set at given T contains N real and $2*N$ complex solutions, we say the fraction of three real roots equals 0 at this temperature point. As shown in Fig. 1, a transition seems to occur around $T_c = 2.1$. For large system size and $T < 2.1$, the solutions for Eq. (19) have only one real root while for $T > 2.1$ they have three real ones. We plot this figure for data length $L = N \times 10^6$, so smaller N means shorter data length, which explains why the curve of $N = 20$ is not quite smooth.

For the iterative method of TAP approximation, we take J^{nMF}, the reconstructed **J** by nMF approximation, as the initial input J^0. Following Eq. (16), we get $J^1, J^2, \ldots$, iteratively. If the change from iteration to iteration $\epsilon(t)$ is

$$\epsilon(t) = \frac{1}{(N-1)^2} \sum_{i,j(i \neq j)} \left| J_{ij}^t - J_{ij}^{t-1} \right|, \qquad (22)$$

less than the threshold value 10^{-5}, then we consider the iteration is convergent and take J_{ij}^t as the result from the iterative method of TAP approximation. There exists an interesting phenomena for the iterative method of TAP. The method is divergent when the solutions of the cubic-equation set contain complex roots but convergent when the solutions are all real roots. Here we mention three possible causes for the divergence. One originates from the frozen states of spin-glass where $m_i^2 = 1$ and neither nMF nor TAP can work. A second possible cause is that there exists a single fixed point of the solution but the initial J_{ij}'s are drawn as J_{ij}^{nMF}, which may be a little bit far away from the true solutions for J_{ij}'s at low T, and the iteration cannot reach the fixed point. The last possible cause may come from the fixed point which is unstable. Here the given results are for $\theta = 0$ and $k = 1$; there are no frozen states for the given temperatures.

We next investigate the influence of T on the reconstruction errors Δ in the case of a zero-external-field ($\theta = 0$) aS-K model ($k = 1$). We plot Δ with T for nMF and TAP in Fig. 2. For TAP approximation, when the iterative method is convergent, it produces the same results (blue triangles) as the cubic-equation method (red circles). Both approximations
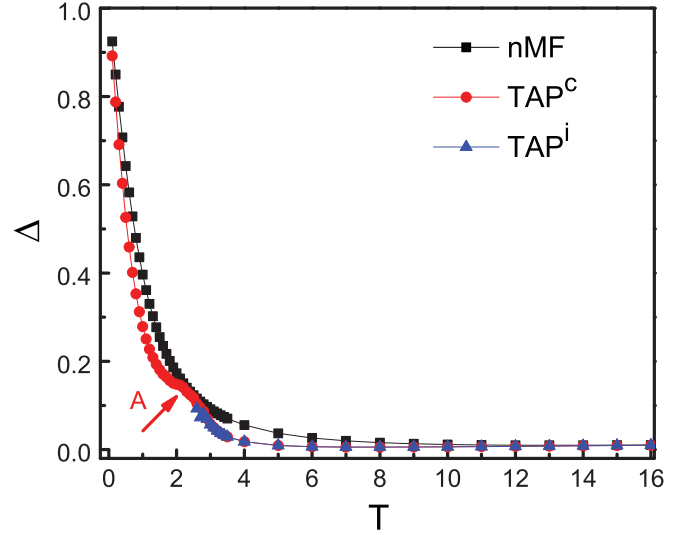

FIG. 2. (Color online) The reconstruction error Δ with temperature T for both nMF and TAP approximation. The other parameter values: $N = 20$, data length $L = 20 \times 10^{10}$, external field $\theta = 0$, asymmetric degree $k = 1$. Black squares, nMF; red circles, cubic equation method for TAP; blue triangles, iterative method for TAP. Each data point is averaged on 10 realizations.

work better with temperature T increasing but approach the same behavior when T goes higher. This is because for Eq. (15) the Onsager term will approach 0 if T goes high enough; that is, there will be no difference between nMF and TAP approximation. As shown in Fig. 2, TAP always works better than nMF before they approach the same results. However, there is a noticeable area in which the curve by the cubic equation method of TAP indicated with the letter "A" is not as smooth as that of nMF. The reason is this temperature interval is located in the critical area where the solutions of the cubic-equation set Eq. (19) represent the coexistence of two states: Some spins have three reals roots and the others have only one real root. We tested also for systems with different sizes and found that larger system size gives more clear inflexions and closer to the critical temperature T_c, around 2.1. Such results are consistent with the results shown in Fig. 1.

Figure 3 illustrates the reconstruction errors for every J_{ij} with scatter plots of the inferred J_{ij}'s by nMF and TAP approximations against J_{ij}^t's. The left plot is for the data length $L = N \times 10^5$ and $L = N \times 10^7$ for the right one. Here, the system size $N = 20$ and the temperature $T = 3.7$ for this plot where the iterative method of TAP is convergent. The scatter plot shows that both nMF and TAP perform better for larger L. As shown in both the left panel and the right panel of Fig. 3, the data points for J_{ij}^{TAP}'s inferred by cubic-equation method are almost covered by that for J_{ij}^{TAP}'s inferred by iterative method, especially for $L = N \times 10^7$.

At last, we see how the data length L works on the reconstruction error Δ in the case of external field $\theta = 0$. For a system with size N, we find the following condition when the data length for asynchronous case L and that for synchronous case L' meet: $L = N * L'$; then the asynchronous update showing comparable behavior (say, Δ versus data length) with that in synchronous case [20]. In Fig. 4, Δ versus L
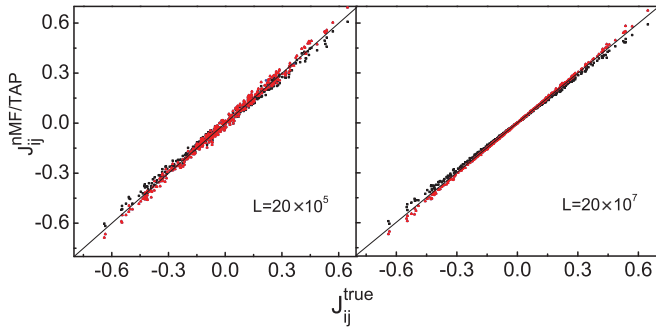
FIG. 3. (Color online) The scatter plot for the reconstructed couplings versus the true ones. The parameter values: $N = 20$, temperature $T = 3.7$, external field $\theta = 0$, asymmetric degree $k = 1$. Black squares, inferred couplings using nMF versus J_{ij}^{true}; blue circles, iterative equation method of TAP versus J_{ij}^{true}; red triangles, cubic method of TAP versus J_{ij}^{true}.

for both nMF and TAP with asynchronous update are plotted at a given temperature $T = 8$, where the iterative method of TAP is convergent. Both nMF and TAP reconstruct better with increasing L; that is, Δ decreases as L increases. For short data length, say, $L < N \times 10^7$, nMF and TAP approximation produce almost the same reconstruction error. However, TAP works better than nMF when $L > N \times 10^8$. Here again we find the data points for cubic-equation method of TAP are covered by those from an iterative method of TAP.

The above results are general to different system size N. The performances for nMF and TAP are also compared with nonzero external field $\theta \neq 0$. We find there exists a frozen state at low testing temperature where neither nMF nor TAP can work.

V. CONCLUSION

We studied the network inference using asynchronously updated kinetic Ising model. Two approximations, nMF and TAP, are introduced to infer the connections and connection strengths in the network. We have found the transition of the solutions' type for the cubic equation method of TAP with critical temperature $T_c \approx 2.1$. We have implemented the TAP approximation as two different schemes: the cubic scheme and the iteration scheme. For a large system, the T_c seems to be the lowest starting temperature point for the TAP iterative method to converge.

Comparing our work with [20], the only difference is the update rules of the Glauber dynamics applied on the aS-K model. The synchronous update is used in [20] while asynchronous update is used in our work. There are two similarities between synchronous and asynchronous update
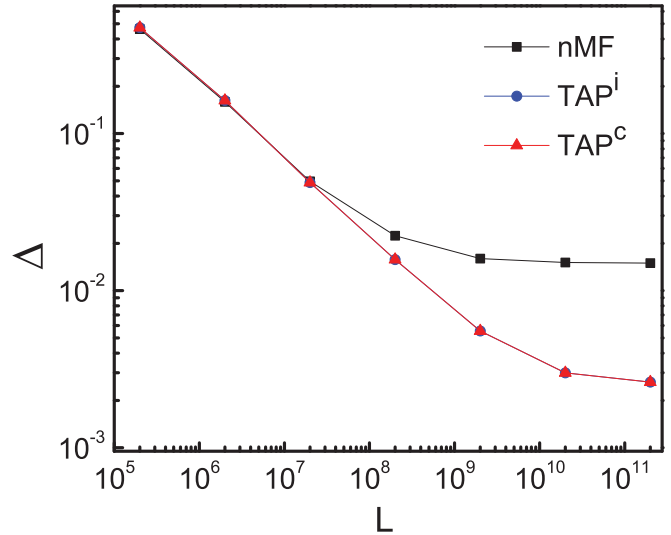

FIG. 4. (Color online) Reconstruction error Δ versus the data length L for nMF and TAP approximation. The other parameter values: $N = 20$, temperature $T = 8$, external field $\theta = 0$, asymmetric degree $k = 1$. Black squares, nMF; blue circles, iterative equation method of TAP; red triangles, cubic method of TAP.

rules. The first one is for both updating rules: nMF and TAP approximation reconstruct better with increasing temperature T or longer data length L. The other one is that TAP works better than nMF with long data length L at given temperatures T. There exist differences between these two update rules also. For instance, the improvement by TAP approximation in the asynchronous case is not as much as that in the synchronous case. Besides, in order to get comparable results with the synchronous case, the data length L for the asynchronous case should be at least N times longer than that for the synchronous case.

This work is able to extend to deal with the biological data from experiments, especially for data produced in continuous time which correspond to the asynchronous updates. Given the large amount of data needed to see a difference, we believe that in most application scenarios, network inference using asynchronously updated kinetic Ising models should work well enough using nMF reconstruction and that the further step to TAP reconstruction would not be needed.

[1] E. R. Alvarez-Buylla *et al.*, Curr. Opin. Plant Biol. **10**, 83 (2007).

[2] K. W. Kohn, Mol. Biol. Cell **10**, 2703 (1999).

[3] L. H. Hartwell, J. J. Hopfield, S. Leibler, and A. W. Murray, Nature (London) **402**, C47 (1999).

[4] U. S. Bhalla and R. Iyengar, Science **283**, 381 (1999).

[5] H. Jeong, B. Tombor, R. Albert, Z. N. Oltvai, and A.-L. Barabasi, Nature (London) **407**, 651 (2000).

[6] Z. Bar-Joseph *et al.*, Nat. Biotechnol. **21**, 1337 (2003).

[7] J. Tegner, M. K. Yeung, J. Hasty, and J. J. Collins, Proc. Natl. Acad. Sci. USA **100**, 5944 (2003).

[8] T. S. Gardner, D. di Bernardo, and D. Lorenz, J. J. Collins, Science **301**, 102 (2003).

[9] S. Cocco, S. Leibler, and R. Monasson, Proc. Natl. Acad. Sci. USA **106**, 14058 (2009).

[10] Y. Roudi, J. A. Hertz, and E. Aurell, Front. Comput. Neurosci. **3**, 1 (2009).

[11] Y. Roudi, S. Nirenberg, and P. E. Latham, PLoS Comput. Biol. **5**, e1000380 (2009).

[12] Y. Roudi, J. Tyrcha, and J. Hertz, Phys. Rev. E **79**, 051915 (2009).

[13] R. J. Prill *et al.*, PLoS One **5**, e9202 (2010).

[14] A. Greenfield, A. Madar, H. Ostrer, and R. Bonneau1, PLoS One **5**, e13397 (2010).

[15] H. Sompolinsky and I. Kanter, Phys. Rev. Lett. **57**, 2861 (1986).

[16] M. V. Feigelman and L. B. Ioffe, Int. J. Mod. Phys. B **1**, 51 (1987).

[17] R. Bausch, H. K. Janssen, R. Kree, and A. Zippelius, J. Phys. C **19**, L779 (1986).

[18] G. Parisi, J. Phys. A **19**, L675 (1986).

[19] J. A. Hertz *et al.*, BMC Neurosci. **11**, 51 (2010).

[20] Y. Roudi and J. Hertz, Phys. Rev. Lett. **106**, 048702 (2011).

[21] F. Greil, B. Drossel, and J. Sattle, New J. Phys. **9**, 373 (2007).

[22] F. Greil and B. Drossel, Phys. Rev. Lett. **95**, 048701 (2005).

[23] K. Klemm, S. Bornholdt, and H. G. Schuster, Phys. Rev. Lett. **84**, 3013 (2000).

[24] E. Schneidman, M. Berry, R. Segev, and W. Bialek, Nature (London) **440**, 1007 (2006).

[25] M. Mezard and T. Mora, J. Physiol. (Paris) **103**, 107 (2009).

[26] E. Marinari and V. V. Kerrebroeck, J. Stat. Mech. (2010) P02008.

[27] E. Aurell, C. Ollion, and Y. Roudi, Eur. Phys. J. B **77**, 587 (2010).

[28] C. E. Shannon, Bell. Syst. Tech. J. **27**, 379 (1948).

[29] M. Suzuki and R. Kubo, J. Phys. Soc. Jpn. **24**, 51 (1968).

[30] R. Glauber, J. Math. Phys. **4**, 294 (1963).

[31] D. J. Thouless, P. W. Anderson, and R. G. Palmer, Philos. Mag. **35**, 593 (1977).

[32] H. J. Kappen and J. J. Spanjers, Phys. Rev. E **61**, 5658 (2000).

[33] Y. Roudi and J. Hertz, J. Stat. Mech. (2011) P03031.